

Received 18 August 2025; revised 13 January 2026; accepted 26 January 2026; date of publication 30 January 2026; date of current version 18 February 2026.

Digital Object Identifier 10.1109/TQE.2026.3659730

# A Quantum Variational Approach to Phase-Only Pattern Synthesis

SIGURD HUBER<sup>1</sup>  AND MICHAEL EPPING<sup>2</sup> 

<sup>1</sup>Microwaves and Radar Institute, German Aerospace Center (DLR), 51147 Cologne, Germany

<sup>2</sup>Institute for Software Technology, German Aerospace Center (DLR), 51147 Cologne, Germany

Corresponding author: Sigurd Huber (e-mail: sigurd.huber@dlr.de).

This work was supported in part by the German Aerospace Center (DLR) Quantum Computing Initiative and in part by the German Federal Ministry of Research, Technology and Space.

**ABSTRACT** Phase-only pattern synthesis is a long-standing and hard to solve problem in antenna engineering. Due to its nonlinear nature, this kind of optimization problem is classically approached with iterative algorithms, where the convergence time depends on the problem topology. Often these heuristic solution routines get stuck in local optima and yield suboptimal results. This article addresses phase-only pattern synthesis by using a variational quantum algorithm, the quantum approximate optimization algorithm. In this context, a mathematical approach is presented, which discretizes the optimization variables and allows representing the original nonlinear functional as a higher order polynomial. In contrast to other series expansion techniques it turns out that this polynomial has finite length without introducing any approximations. This makes phase-only patterns synthesis problems suitable to be solved on quantum computers with standard gate sets. The mathematical treatment of this optimization problem is complemented by a complexity analysis and a performance analysis. Finally, the challenges regarding future deployment of quantum approximate optimization for phase-only pattern synthesis are discussed.

**INDEX TERMS** Antenna pattern optimization, phase-only pattern synthesis, quantum approximate optimization algorithm (QAOA), quantum approximate optimization, variational quantum algorithms.

## I. INTRODUCTION

Phase-only pattern synthesis is an optimization concept where the elements of an antenna array are controlled via phase-shifters in order to generate a predefined radiation field. Although this optimization technique could in principle be applied to antennas in receive mode, the main motivation is to operate the transmit amplifiers of an antenna in saturation, ensuring a maximum of radiated power. This method dates back as far as to the 1960s and 1970s [14], [19], [30], [34] and is of relevance still today. For instance, modern synthetic aperture radar (SAR) systems for Earth observation heavily rely on phase-only pattern optimization for the design of powerful SAR imaging modes [3], [27], [46], [53].

Phase-only pattern synthesis falls into the class of nonlinear optimization, which means that classically these kind of problems are approached with iterative methods. There exists already a plethora of optimization approaches for various types of multielement antennas. For example, the authors in [11] and [12] introduced a vector-Newton algorithm and an iterative gradient method for null-steering, respectively. Other gradient-based approaches are presented in [25] with

a nonlinear constrained optimization structure and in [47] under the name ‘conjugate gradient method’. Several algorithms have been investigated for linear and planar array antennas [15], [16] with the goal to minimize sidelobe levels for interference mitigation. Phase-only patterns synthesis extended to other antenna types has been reported in [7] for array-fed reflectors and in [6] and [8] for conformal arrays. The latter paper presents the synthesis problem as an intersection finding problem, which is solved by means of a generalised projection algorithm. A generalization to linear aperture patterns can be found in [52]. With the availability of increasingly more powerful computers, Fourier domain methods are proposed, such as in [33], where an iterative method using Fourier analysis for planar phased arrays is presented. In [10], phase-only pattern synthesis based on an advanced fast Fourier transform algorithm for reflect-arrays is investigated. A further generalization based on Fourier calculus is the nonuniform fast Fourier transform, which has been exploited in the context of conformal reflect-arrays [9]. Other concepts in adaptive interference rejection for linear phased arrays foresee the use of weighted basis functions [18], the

minimization of a nonlinear functional using an iterative method [26] or a stochastic gradient descent approach [5]. An iterative projection method for a dynamical reconfiguration of the antenna pattern is introduced in [24], a modified least squares method in [42] and phase-only pattern synthesis solved via an alternating direction method of multipliers in [31] and the exploitation of a spline-based parameterization is analyzed in [43].

Quantum computing has been discovered for antenna optimization and related fields rather recently. As a new paradigm, quantum computing is interesting in particular for antenna optimization, because it allows in principle finding global optima. Classically, even sophisticated solvers are not guaranteed to find global optima, due to their fundamental limitation to compute on a small fraction of the solution space. In contrast, quantum computers are able to exploit superpositions, which allows a proven quantum speedup in specific cases [20].

First approaches to optimize antennas mimic quantum mechanical effects as in [37] where a quantum inspired version of particle swarm optimization for linear array antenna synthesis and other problems in electromagnetics is presented. Another application of quantum computing to antenna design is presented in [13], where a quantum inspired genetic algorithm is considered. An example where a classical solver for semidefinite programs has been transferred to a quantum version is presented in [4] and offers a square-root speed-up over its classical pendants. In the context of antenna array thinning Rocca et al. [44] presented a method exploiting the quantum Fourier transform (QFT), while Tosi and Rocca [50] treated this problem in the frame of the quantum approximate optimization algorithm (QAOA). A further application of the QFT to antenna pattern analysis is introduced in [51]. A research field related to antenna optimization is multiple-input multiple-output systems in communications. In [29], a signal-to-noise ratio optimization problem is formulated as a combinatorial optimization problem to be solved on a quantum annealer. Concepts of adiabatic quantum computation, and in particular quantum annealing, applied to array processing have been investigated in [22] and [49], where for instance problems encountered in digital beamforming are addressed. Further examples, where quantum annealing and annealing-inspired approaches turn out to be promising, are for the optimization of reflective metasurfaces [32], [45], [54]. A first example of phase-only pattern synthesis is formulated as a Grover search [20] problem in [23], where an oracle quantum circuit is used to evaluate the objective function.

A specific challenge in phase-only pattern synthesis is that one deals with continuous variables. By discretizing these variables, at first glance this seems like making a complicated problem even more complicated. But in many real-world antenna optimization problems, such as in SAR Earth observation, transmit/receive modules for antenna systems are equipped with digital phase controllers [39]. Insofar it is natural to employ a discrete encoding of the optimization

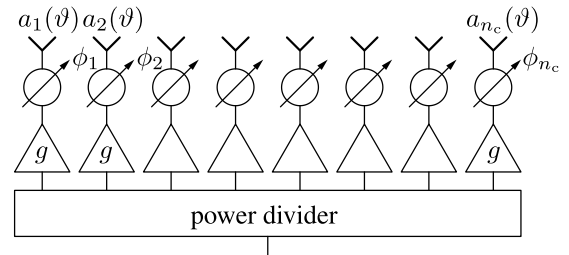


**FIGURE 1.** Array antenna block diagram with phase shifters ( $\phi_i$ ) generating a desired radiation field. The amplification factors  $g$  of the individual antenna elements are kept constant.

variables. In this work, we present phase-only pattern synthesis as combinatorial optimization problem to be solved in the frame of variational quantum algorithms and in particular the QAOA, first introduced in [17].

## II. PROBLEM STATEMENT

As an optimization technique, phase-only pattern synthesis can be applied to a wide variety of antenna types and topologies. The concept drawing in Fig. 1 shows a linear array antenna, where the individual antenna elements or channels are controlled via phases  $\phi_i$ ,  $i \in [1, n_c]$  where  $n_c$  is the number of channels. The factor  $g$  represents constant amplification, which we set to one for the purpose of the mathematical problem formulation. Each element is identified by a unique pattern function  $a_i$ , which represents the electromagnetic far field produced by this emitter. In standard phased array antennas, this pattern function is often called the steering vector, which is the product of the space factor and the array factor. In an array-fed reflector antenna this function would be the secondary pattern. In general, these far field patterns depend on two spherical angles and the frequency. It is important to note that these kind of pattern optimization problems are usually considered in the so called narrow band approximation, although there is no principal restriction to extend this optimization to the frequency domain. Here, for notational simplicity, the second angular variable is omitted as well as the frequency variable, which is assumed constant in the subsequent problem treatment.

Under the above assumptions the total radiated field  $\sum_i w_i a_i(\vartheta)$  is a linear combination of the individual antenna pattern far field functions and some complex weights  $w_i$ , also called excitation coefficients. The optimization of the radiation pattern is performed on the gain function  $G(\vartheta)$  which can be written as

$$G(\vartheta) = \frac{1}{P_{\text{rad}}} \left| \sum_{i=1}^{n_c} w_i a_i(\vartheta) \right|^2 \quad w_i, a_i \in \mathbb{C} \quad (1)$$

with the radiated power

$$P_{\text{rad}} \propto \sum_{i=1}^{n_c} |w_i|^2. \quad (2)$$

For phase-only pattern synthesis these complex weights can be expressed according to

$$w_i = e^{i\phi_i} \quad (3)$$

such that the  $\phi_i$  are the only optimization variables. In this case the radiated power of a phased-array antenna is constant, proportional to the number of antenna elements

$$P_{\text{rad}} \propto n_c. \quad (4)$$

This allows formulating an optimization problem

$$\underset{\phi_i}{\text{minimize}} \quad \sum_l \gamma_l (G - \tilde{G})^2 (\vartheta_l) \quad (5)$$

where the summed quadratic deviation of the desired gain pattern  $G$  from a target gain pattern  $\tilde{G}$  is minimized. The counting index  $l$  indicates that the angular coordinate  $\vartheta$  is taken at discrete positions, which should obey spatial sampling rules in order to avoid unwanted pattern distortions, for instance in undersampled angular regions. The coefficients  $\gamma_l$  represent a heuristic weighting function, which allows balancing the disparity in cost function magnitudes for certain domains, e.g. pattern sidelobe versus pattern mainlobe regions. Substituting (1) and (4) into the cost function in (5) and multiplying with the number of channels  $n_c$  gives

$$\underset{\phi_i}{\text{minimize}} \quad \sum_l \gamma_l \left( \left| \sum_i w_i a_i \right|^2 - n_c \tilde{G} \right)^2 (\vartheta_l). \quad (6)$$

Considering the weights according to (3), the task of minimizing the quadratic pattern deviation represents a nonlinear optimization problem over a set of real-valued antenna channel phases  $\phi_i \in [0, 2\pi)$ .

### III. QUANTUM COMPUTATIONAL FORMALISM

In quantum optimization, the values of the cost function can be interpreted as the energy eigenvalues  $e_\mu$  of some cost or problem Hamiltonian  $H_p$ , to be defined below. Expanding the functional in (5) consequently yields

$$e_\mu = \sum_l \gamma_l \left( \sum_{ijmn} w_i w_j^* w_m w_n^* a_{il} a_{jl}^* a_{ml} a_{nl}^* - 2 \sum_{ij} w_i w_j^* a_{il} a_{jl}^* n_c \tilde{G}_l + n_c^2 \tilde{G}_l^2 \right). \quad (7)$$

The challenge one faces with phase-only pattern synthesis is that this nonlinear optimization problem needs to be converted to a form accessible to a quantum computer. By introducing a proper discretization of the antenna channel phases  $\phi_i$  it turns out that this problem can be written as a higher order polynomial, which can be represented by so called spin glass Hamiltonians. With a discretization according to

$$\phi_i = \frac{2\pi}{2^{n_b}} \sum_{k=0}^{n_b-1} 2^k x_{ik} \quad (8)$$

$n_b$  bits each are used to represent  $2^{n_b}$  phases from the interval  $[0, 2\pi)$  as function of binary variables  $x_{ik} \in \{0, 1\}$ . A short calculation, substituting expression (8) into (3), yields

$$\begin{aligned} w_i &= e^{i\phi_i} = e^{i \frac{2\pi}{2^{n_b}} \sum_{k=0}^{n_b-1} 2^k x_{ik}} = \prod_{k=0}^{n_b-1} e^{i2\pi 2^{k-n_b} x_{ik}} \\ &= \prod_{k=0}^{n_b-1} \sum_{m=0}^{\infty} \frac{1}{m!} (i2\pi 2^{k-n_b} x_{ik})^m \\ &= \prod_{k=0}^{n_b-1} \left[ 1 + x_{ik} \sum_{m=1}^{\infty} \frac{1}{m!} (i2\pi 2^{k-n_b})^m \right] \\ &= \prod_{k=0}^{n_b-1} \left[ 1 + x_{ik} (e^{i2\pi 2^{k-n_b}} - 1) \right]. \end{aligned} \quad (9)$$

In the series expansion of the exponential function the case distinction

$$x^m = \begin{cases} 1, & m = 0 \\ x, & m > 0 \end{cases} \quad (10)$$

with  $0^0 = 1$  has been exploited. For instance, for  $n_b = 3$  bit phase quantization we have a third order polynomial

$$\begin{aligned} w_i &= \left[ 1 + x_{i0} (e^{i2\pi 2^{-3}} - 1) \right] \left[ 1 + x_{i1} (e^{i2\pi 2^{-2}} - 1) \right] \\ &\quad \times \left[ 1 + x_{i2} (e^{i2\pi 2^{-1}} - 1) \right]. \end{aligned} \quad (11)$$

It is now straight forward to write the weights  $w_i$  in terms of spin variables  $s_{ik} \in \{1, -1\}$ , which are related to the binary variables  $x_{ik}$  according to

$$x_{ik} = \frac{1}{2}(1 - s_{ik}). \quad (12)$$

Inserting (12) into the formula for the excitation coefficients (9) finally yields

$$\begin{aligned} w_i &= \prod_{k=0}^{n_b-1} \frac{1}{2} \left[ (e^{i2\pi 2^{k-n_b}} + 1) - s_{ik} (e^{i2\pi 2^{k-n_b}} - 1) \right] \\ &= \prod_{k=0}^{n_b-1} e^{i\pi 2^{k-n_b}} [\cos(\pi 2^{k-n_b}) - i s_{ik} \sin(\pi 2^{k-n_b})] \\ &= e^{i\pi(1-2^{-n_b})} \prod_{k=0}^{n_b-1} [\cos(\pi 2^{k-n_b}) - i s_{ik} \sin(\pi 2^{k-n_b})]. \end{aligned} \quad (13)$$

As a result, the functional (7) together with the expression for the weights (13) define a higher order polynomial in the spin variables  $s_{ik}$  and shall serve as basis for the derivation of a quantum circuit using the QAOA.

#### A. HAMILTONIAN REPRESENTATION

Solving such a minimization problem with the quantum approximate optimization problem means encoding the functional (7) in a proper Hamiltonian, which shall be referred to

as the problem Hamiltonian  $H_p$ . Cost functions, which can be written as polynomials, can be represented by so called spin glass Hamiltonians. The variable encoding the problem would be the magnetic spin  $s$  and to every eigenstate of this particular problem Hamiltonian corresponds an eigenvalue, which may be written in a general form as

$$e_\mu = \sum_{j_1, j_2, \dots, j_n=0}^r \tilde{c}_{j_1 j_2 \dots j_n} s_1^{j_1} s_2^{j_2} \dots s_n^{j_n}. \quad (14)$$

For our particular optimization problem the highest power  $r$  for an individual spin variable is four, which can be seen by inserting the weights in the spin basis (13) into the term  $w_i w_j^* w_m w_n^*$  in (7). In total  $n = n_c n_b$  spins or qubits are required in order to encode an antenna optimization problem with  $n_c$  antenna channels and  $n_b$  bits for the phase quantization in each channel. The coefficients  $\tilde{c}$  are associated with the coefficients of the terms when expanding the cost function (7) including the weights (13). At this point the powers in the polynomial (14) may be reduced using

$$s^j = \begin{cases} 1, & j \in 2\mathbb{N} \\ s, & j \in 2\mathbb{N} + 1 \end{cases} \quad (15)$$

which yields

$$e_\mu = \sum_{i_1, i_2, \dots, i_n=0}^1 c_{i_1, i_2, \dots, i_n} s_1^{i_1} s_2^{i_2} \dots s_n^{i_n}. \quad (16)$$

The new coefficients  $c$  are given as

$$c_{i_1, i_2, \dots, i_n} = \sum_{j_1, j_2, \dots, j_n \bmod 2} \tilde{c}_{j_1 j_2 \dots j_n} \quad (17)$$

where the modulo operation acts on each index  $j_v$  individually.

The spin variables  $s$  are the eigenvalues of the Pauli-z-matrix  $\sigma^z$ , so that the problem Hamiltonian can be expressed as

$$H_p = \sum_{i_1, i_2, \dots, i_n=0}^1 c_{i_1 i_2 \dots i_n} (\sigma_1^z)^{i_1} \otimes (\sigma_2^z)^{i_2} \otimes \dots \otimes (\sigma_n^z)^{i_n}. \quad (18)$$

In this formulation it is understood that each Pauli operator acts on a specific qubit, indicated by the subscript numbers. The time evolution operator is computed by exponentiation of the problem Hamiltonian and replacing the time variable in the Trotterization step by general parameters  $\beta_t$  to be found by classical optimization. Then, the problem unitary may be written according to (see Appendix A)

$$\begin{aligned} U_p(\beta_t) &= e^{-i\beta_t H_p} \\ &= \prod_{i_1, i_2, \dots, i_n=0}^1 \left[ \cos(\beta_t c_{i_1 i_2 \dots i_n}) \bigotimes_{v=1}^n I \right. \end{aligned}$$

$$\left. - i \sin(\beta_t c_{i_1 i_2 \dots i_n}) \bigotimes_{v=1}^n (\sigma_v^z)^{i_v} \right] \quad (19)$$

with  $I$  the single qubit identity operator. Together with the initial or mixer Hamiltonian

$$H_0 = \sum_{i=1}^n \bigotimes_{v=1}^n (\sigma_v^x)^{\delta_{vi}} \quad (20)$$

defining the corresponding unitary

$$\begin{aligned} U_0(\alpha_t) &= e^{-i\alpha_t H_0} \\ &= \prod_{i=1}^n \left[ \cos(\alpha_t) \bigotimes_{v=1}^n I \right. \\ &\quad \left. - i \sin(\alpha_t) \bigotimes_{v=1}^n (\sigma_v^x)^{\delta_{vi}} \right] \end{aligned} \quad (21)$$

the phase-only pattern synthesis problem is completely represented in the frame of the QAOA with the  $t$ th iteration  $U_0(\alpha_t)U_p(\beta_t)$ .

## B. CIRCUIT DESIGN

Each factor in the problem unitary (19) is represented by a sub-circuit. Here, as an illustrative example, we derive the quantum circuit for a unitary describing a third order polynomial

$$U_p(\beta_t) = \cos(\beta_t c_{111}) I \otimes I \otimes I - i \sin(\beta_t c_{111}) Z \otimes Z \otimes Z \quad (22)$$

where the Pauli-matrices  $\sigma^z$  have been replaced by the usual symbol in quantum circuit design

$$Z = \begin{pmatrix} 1 & 0 \\ 0 & -1 \end{pmatrix}. \quad (23)$$

In order to obtain an efficient quantum circuit composed of native operations, such as controlled-not gates (CNOTs) and the rotation gate

$$R^z(\theta) := e^{-i\theta/2Z} = \begin{pmatrix} e^{-i\theta/2} & 0 \\ 0 & e^{i\theta/2} \end{pmatrix} \quad (24)$$

the unitary (22) needs to be brought into the form

$$\begin{aligned} &\cos(\beta_t c_{111}) I \otimes I \otimes I - i \sin(\beta_t c_{111}) Z \otimes Z \otimes Z \\ &= U [\cos(\beta_t c_{111}) I \otimes I \otimes I - i \sin(\beta_t c_{111}) Z \otimes I \otimes I] U^\dagger \\ &= U [R^z(2\theta) \otimes I \otimes I] U^\dagger. \end{aligned} \quad (25)$$

This is true for the unitary  $U$  representing a series of two CNOT-gates

$$\begin{aligned} &(I \otimes I \otimes |0\rangle\langle 0| + X \otimes I \otimes |1\rangle\langle 1|) \cdot \\ &(I \otimes |0\rangle\langle 0| \otimes I + X \otimes |1\rangle\langle 1| \otimes I) \\ &= \text{CNOT}(3, 1) \cdot \text{CNOT}(3, 2) \end{aligned} \quad (26)$$

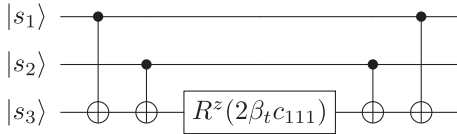


**FIGURE 2.** Quantum circuit implementing the third order polynomial  $c_{111}s_1s_2s_3$ .

where in the notation CNOT(3, 1) the first number denotes the control qubit and the second number the target qubit. Here, X denotes the Pauli X gate (the NOT gate). Since the CNOT gates involved here commute, the unitary of the entire quantum subcircuit may be written as

$$\begin{aligned} & \text{CNOT}(3, 1) \cdot \text{CNOT}(2, 1) \cdot (R^z \otimes I \otimes I) \cdot \\ & \text{CNOT}(2, 1) \cdot \text{CNOT}(3, 1) \end{aligned} \quad (27)$$

with the corresponding circuit block diagram shown in Fig. 2 (see [40] paragraph 4.7.3).

Due to the permutation symmetry the qubit labels, i.e. the role of the qubits in the circuit, can be swapped without altering the action of the whole subcircuit. This design pattern can be used as a building block in larger circuits.

Constructing the quantum circuit for the entire problem unitary (19) by a sequence of subcircuits with a form as presented in Fig. 2 may benefit to a certain degree from optimization [41]. For example subcircuits acting on different subsets of qubits  $s_v$  could be executed simultaneously, resulting in a lower circuit depth (see Appendix B). However, the overall circuit complexity is still determined by the number of unique terms  $n_t$  in the problem polynomial (7).

### C. COMPLEXITY ANALYSIS

Determining this number is not a trivial task. Not only the reduction in the number of terms due to (15) needs to be taken into account, but also the permutation symmetry of the summation indices over the antenna channels  $i, j, m$ , and  $n$  in the cost function (7) as well as the fact that the cosine-terms in the expression for the excitation coefficients (13) vanish for  $k = n_b$ .

Disregarding these term-reducing aspects for now and expanding, for example, the expression  $w_i w_j^*$  in (7) by substituting (13) yields

$$\begin{aligned} w_i w_j^* &= \prod_{k=0}^{n_b-1} [\cos(\pi 2^{k-n_b}) - i s_{ik} \sin(\pi 2^{k-n_b})] \\ &\quad \cdot [\cos(\pi 2^{k-n_b}) + i s_{jk} \sin(\pi 2^{k-n_b})]. \end{aligned} \quad (28)$$

According to the multinomial theorem this product of sums can be converted into a sum of products. Then, by multiplying the summation limits an upper bound for the number of terms can be determined as

$$n_t = n_c^4 2^{4n_b} + n_c^2 2^{2n_b} + 1. \quad (29)$$

**TABLE 1.** Number of Terms  $n_t$  in the Cost Function (7) for a Given Number of Channels  $n_c$  and Bits Per Channel  $n_b$

$n_c \backslash n_b$	1	2	3	4	5	6
1	1	1	1	1	1	1
2	2	6	21	81	321	1281
3	4	28	157	1009	7105	52993
4	8	95	761	7649	92033	1252865
5	16	251	2441	28961	392321	5747201
6	31	556	6061	78001	1110721	16730881

On the other hand, by inspecting the Hamiltonian representation (16), the number of terms can be at most

$$2^n = 2^{n_c n_b}. \quad (30)$$

Sofar these results tell us little about how much the number of terms reduce under the above mentioned conditions. An exact evaluation, using symbolic calculation tools, yields the numbers of terms as presented in Table 1 as function of the number of channels and the number of bits used to quantize the phases of the excitation coefficients. At this point it is important to stress that in modern antenna design and optimization the number of antenna channels plays a far more important role as the quantization of the channel phases. Typical phase quantization on spaceborne Earth observation satellites is realized with 6 bits per channel [1], [21], [48]. Insofar, it is important to know how the number of terms scale with larger number of antenna channels  $n_c$ . Here, we notice first that, based on the permutation symmetry of the summation indices, the terms in expressions such as  $\sum_{ijmn} w_i w_j^* w_m w_n^* \sum_l a_{il} a_{jl}^* a_{ml} a_{nl}^*$  can be interpreted as components of a symmetric tensor. An  $m$ th order tensor with  $n$  elements in each index would have  $\binom{n+m-1}{m}$  unique components, which, adapted to our case, would yield

$$\binom{n_c + 3}{4} = \frac{1}{4!} (n_c + 3)(n_c + 2)(n_c + 1)n_c \quad (31)$$

unique terms. With this observation and from inequality (29) one can conclude that the number of terms for a given number of bits can be expanded into a fourth-order polynomial in the number of channels

$$n_t = 1 + p_1(n_b)n_c + p_2(n_b)n_c^2 + p_3(n_b)n_c^3 + p_4(n_b)n_c^4 \quad (32)$$

with rational coefficients  $p_j \in \mathbb{Q}$ ,  $j \in \{1, 2, 3, 4\}$ . For a single-channel antenna the number of terms is independent from the phase-quantization. This can be verified by inspecting the gain expression according to (1), which becomes a phase-independent constant, implying a total number of terms of exactly one. These coefficients have been calculated for a number of bits of up to six (see Table 2). As a final observation, the progression of the coefficients  $p_4$  in the last column in Table 2 suggests that it follows an exponential increase  $2^{4(n_b-1)}$ . Therefore, the last term in the polynomial (32) takes the form

$$p_4(n_b)n_c^4 = \frac{1}{4!} 2^{4(n_b-1)} n_c^4. \quad (33)$$

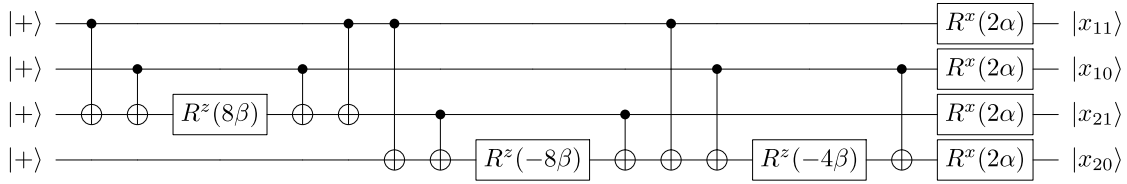


**FIGURE 3.** Example implementation of the QAOA solving the problem Hamiltonian (37) for our phase-only pattern synthesis demonstration problem (35). The parameters  $\alpha$  and  $\beta$  are found via classical optimization. The optimization result is encoded in the binary string represented by the output state vector  $|x_{11}x_{10}x_{21}x_{20}\rangle$ .

**TABLE 2.** Coefficients of the Fourth-Order Polynomials That Give the Number of Terms  $n_t$  for Fixed Precision  $n_b$

$n_b$	$4!p_1$	$4!p_2$	$4!p_3$	$4!p_4$
1	-18	23	-6	1
2	-60	92	-48	16
3	-1008	1904	-1152	256
4	-19392	36800	-21504	4096
5	-347904	651008	-368640	65536
6	-5913600	10959872	-6094848	1048576

This aligns with our estimate of the upper bound of the number of terms given in (29) and confirms the complexity of the quantum circuit for our phase-only patterns synthesis problem to be

$$\mathcal{O}(n_c^4 2^{4n_b}). \quad (34)$$

#### IV. DEMONSTRATION EXAMPLE

To give the reader an impression of the performance of quantum-assisted phase-only pattern synthesis, in the following a short demonstration example shall be presented. It is inspired by a similar toy problem discussed in [23], which uses two antenna channels, each with two bit phase quantization. Adapted to our problem formulation according to (6) this expression takes the form

$$\text{minimize}_{\phi_1, \phi_2} \left( \left| e^{i(\phi_1 + \bar{\phi}_1)} + e^{i(\phi_2 + \bar{\phi}_2)} \right|^2 - n_c \tilde{G} \right)^2 \quad (35)$$

with  $\bar{\phi}_1 = \pi/2$ ,  $\bar{\phi}_2 = \pi$  and the target gain  $\tilde{G} = 2$ . Moreover, we have chosen only a single direction  $\vartheta_l$  as it does not affect the mathematical problem structure. Note that each antenna element pattern phase  $\bar{\phi}_l$  corresponds to an angle  $\vartheta_l$ . Referring to the notation used in (6) this would mean that the antenna element patterns  $a_1$  and  $a_2$  would simply take the form  $e^{i\bar{\phi}_1} = i$  and  $e^{i\bar{\phi}_2} = -1$ , respectively.

Evaluating (7) substituting (13) yields the corresponding cost function in the spin basis (16)

$$e_\mu = 4s_{11}s_{10}s_{21} - 4s_{11}s_{21}s_{20} - 2s_{10}s_{20} + 6. \quad (36)$$

That the number of terms is four instead of six as listed in Table 1 is a consequence of our particular choice of antenna parameters, which yielded a cancellation of two terms.

This functional can now be translated into the problem Hamiltonian (18)

$$H_p = 4\sigma^z \otimes \sigma^z \otimes \sigma^z \otimes \mathbf{I} - 4\sigma^z \otimes \mathbf{I} \otimes \sigma^z \otimes \sigma^z - 2\mathbf{I} \otimes \sigma^z \otimes \mathbf{I} \otimes \sigma^z + 6\mathbf{I} \otimes \mathbf{I} \otimes \mathbf{I} \otimes \mathbf{I} \quad (37)$$

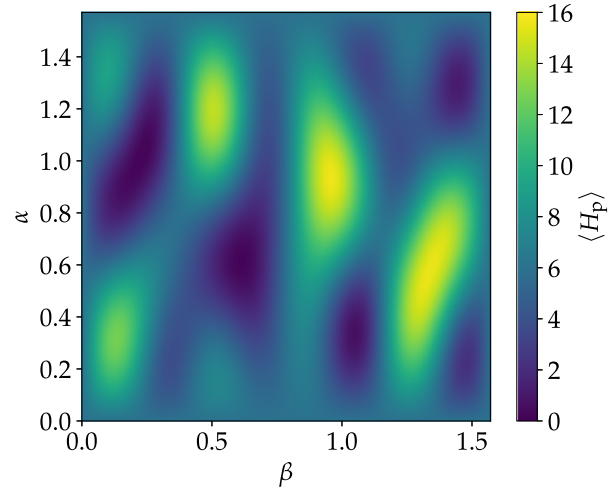


**FIGURE 4.** Expectation value ( $H_p$ ) of the problem Hamiltonian as function of the parameters  $\alpha$  and  $\beta$ .

with the corresponding quantum circuit shown in Fig. 3.

In the construction of this quantum circuit we have used the standard definition of the rotation operator about the  $x$ -axis according to

$$R^x(\theta) := e^{-i\theta/2X} = \begin{pmatrix} \cos(\theta/2) & -i \sin(\theta/2) \\ -i \sin(\theta/2) & \cos(\theta/2) \end{pmatrix}. \quad (38)$$

The parameters  $\alpha$  and  $\beta$  are found iteratively by classical optimization routines via an hybrid approach with alternating classical and quantum calculations. Here, for our demonstration example it is possible to compute the analytical expression of the expectation value of the problem Hamiltonian according to

$$\begin{aligned} \langle H_p \rangle &= \sin(2\alpha) \left( 8 \cos^2(2\alpha) \sin(16\beta) - \sin(2\alpha) \cos(16\beta) \right. \\ &\quad \left. + 4 \sin(4\beta) (2 \sin(4\alpha) \sin(8\beta) + \cos(2\alpha) \cos(8\beta)) \right) \\ &\quad + \frac{1}{2} \cos(4\alpha) (8 \sin(2\alpha) (\sin(4\beta) + \sin(12\beta)) - 1) \\ &\quad + \frac{13}{2}. \end{aligned} \quad (39)$$

This expectation value has been evaluated over a range of values  $\alpha$  and  $\beta$  between 0 and  $\pi/2$ , after which the energy landscape repeats itself periodically (see Fig. 4). With the optimal set of parameters, which are found to be  $\alpha = \beta \approx 0.6157$ , a simulation of the quantum circuit under error-free conditions

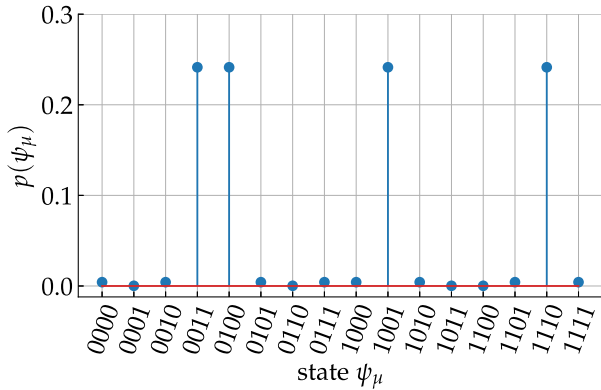


**FIGURE 5.** Simulated output state vector, with four solutions indicated by equally high measurement probabilities. The solutions are encoded in the decimal representation of the eigenstates (see Table 3).

**TABLE 3.** Four Optimal Solution Sets  $\phi_1$  and  $\phi_2$ , Represented as Binary Bit-Strings Labeling the Corresponding Basis Vectors

state binary	$\phi_1$	$\phi_2$
0 0 1 1	$0^\circ$	$270^\circ$
0 1 0 0	$90^\circ$	$0^\circ$
1 0 0 1	$180^\circ$	$90^\circ$
1 1 1 0	$270^\circ$	$180^\circ$

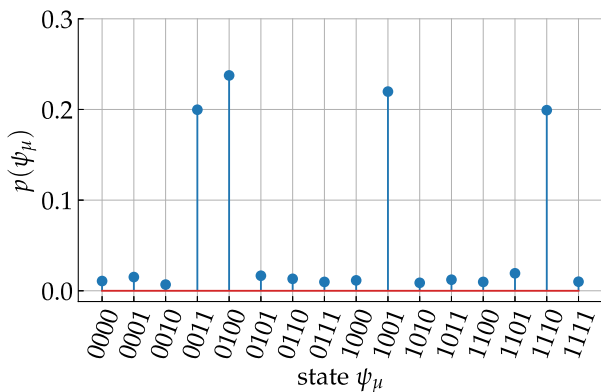


**FIGURE 6.** Output state vector as measured on the IBM Torino quantum computer.

yields the output state probabilities as presented in Fig. 5. The decimal numbers represent binary bit-strings that encode the antenna channel phases according to (8). A first observation is that we have four equally probable solutions, which is clearly a consequence of the two-bit quantization of the channel phases and the fact that a global phase can be extracted in (35). These four solutions yield the minimal value ( $e_\mu = 0$ ) of the cost function (36) and correspond to the eigenvalues of the ground state of the problem Hamiltonian. Table 3 lists the decimal, binary and angular representation of these solutions, which appear with a probability of 24.14%. The next higher eigenstates ( $e_\mu = 4$ ) are measured with 0.42% probability, while the highest eigenstates ( $e_\mu = 16$ ) have 0.019% probability.

For comparison, in Fig. 6 the results are presented, when the quantum circuit (see Fig. 3) for our demonstration

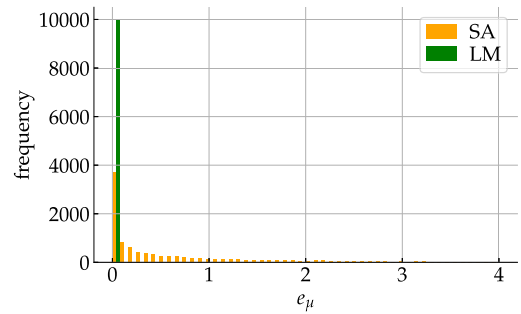


**FIGURE 7.** Histogram of the objective values for the LM algorithm and SA. The global minimum lies at  $e_\mu = 0$ .

problem is executed on real quantum hardware. The output state has been sampled 4096 times on the IBM Torino quantum computer with a Heron r1 processor, featuring 133 qubits. In contrast to the results under ideal conditions given in Fig. 5, individual solutions occur now with probabilities between 19.9% and 23.8%, while individual nonsolutions appear in between 0.7% and 1.9% of the cases.

## V. PERFORMANCE COMPARISON

Phase-only pattern synthesis in the conventional sense is an optimization problem over continuous variables  $\phi_i \in [0, 2\pi)$ . The quantum variational approach suggested here, is based on a discretization of the optimization variables  $\phi_i$  and treats the original problem as combinatorial optimization. This means not only the optimization approach is quite different but also the problem topology itself, which might impact the optimization performance.

The classical solvers, to be compared against, are a damped Gauss-Newton approach, known as Levenberg–Marquardt (LM) algorithm [35], [38], and simulated annealing (SA) [28], [36], which exploits concepts of statistical mechanics for combinatorial optimization.

The next more complicated application example, which shall serve as benchmark problem, is of the same structure as given in the previous example according to (35) but with four antenna channels. In this case the antenna element patterns  $a_i$  have been chosen as  $[i \ -i \ 1]$  and the target gain  $\tilde{G}$  to be 4. The minimum objective value  $e_\mu$ <sup>1</sup> of this optimization example is again 0. Note, for the classical approaches the original problem with continuous optimization variables has been solved. Fig. 7 shows the histogram of the objective values that the classical solvers found with a total of  $10^4$  trials. In this particular example, the LM algorithm was able to find the global optimum in 100% of the trials, while SA succeeded in 37.2% of the cases.

Phase-only pattern synthesis via quantum approximate optimization has been implemented using a classical solver, namely, SA, which takes the expectation value of the problem Hamiltonian  $\langle H_p \rangle$  as an input. With 2-bit quantization of

<sup>1</sup>In the context of these classical optimization approaches  $e_\mu$  shall be interpreted as continuous function.

**TABLE 4. Four Optimal Solution Sets  $\phi_1$  to  $\phi_4$  in Binary and in Decimal Representation**

state binary	state decimal	$\phi_1$	$\phi_2$	$\phi_3$	$\phi_4$
0 0 1 1 1 0 0 1	57	$0^\circ$	$270^\circ$	$180^\circ$	$90^\circ$
0 1 0 0 1 1 1 0	78	$90^\circ$	$0^\circ$	$270^\circ$	$180^\circ$
1 0 0 1 0 0 1 1	147	$180^\circ$	$90^\circ$	$0^\circ$	$270^\circ$
1 1 1 0 0 1 0 0	228	$270^\circ$	$180^\circ$	$90^\circ$	$0^\circ$

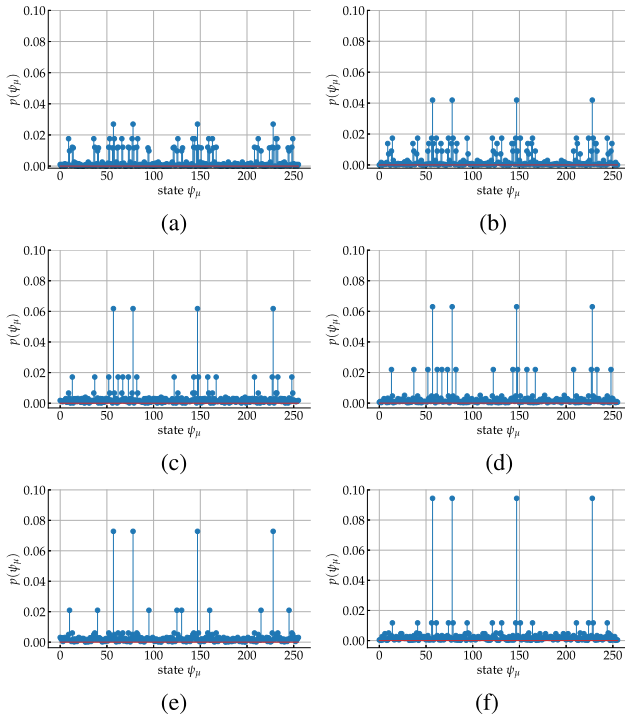


**FIGURE 8. Final output states after hybrid optimization for different QAOA-layer numbers  $n_1$ . The total probability to find an optimal solution is denoted by  $p_o$ . (a)  $n_1 = 1$  and  $p_o = 10.78\%$ . (b)  $n_1 = 2$  and  $p_o = 16.78\%$ . (c)  $n_1 = 3$  and  $p_o = 24.73\%$ . (d)  $n_1 = 4$  and  $p_o = 25.2\%$ . (e)  $n_1 = 5$  and  $p_o = 29.12\%$ . (f)  $n_1 = 10$  and  $p_o = 37.76\%$ .**

the phases, this optimization problem has again four solutions (see Table 4), all corresponding to the minimum energy level  $e_\mu = 0$ . For the four element patterns introduced above and 2-bit phase quantization, the cost function possesses 51 unique terms after contraction of terms with the same powers. Fig. 8 shows the final probability amplitudes of the output state after hybrid optimization. The different subplots present the results for different numbers of QAOA-layers  $n_1$ . The total probability  $p_o$  to find the global optimum increases from 10.78% for the single-layer case to 37.76% for ten layers. As expected from the symmetry, all four solutions appear with the same probability, regardless of the number of layers.

It is instructive to expand the analysis for the classical optimization approaches to a real-world example. In the following, the TerraSAR-X antenna [48], featuring 32 channels, shall be considered. Here, the goal was to widen the main-beam while setting sidelobe level constraints 18.5 dB below the mainlobe [see Fig. 9(a)]. In addition, a weighting  $\gamma_l$  of 50 of the objective function [see (5)] in the sidelobes has been

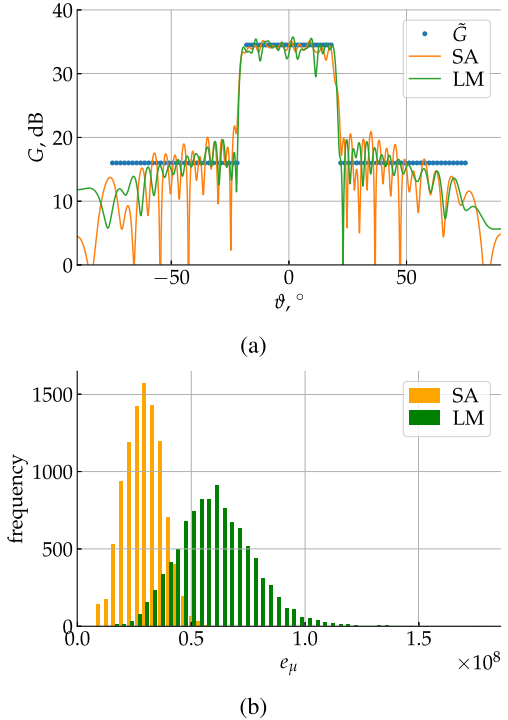


**FIGURE 9. (a) Optimized antenna patterns with SA and the LM algorithm. The blue dots represent the target gain pattern  $\tilde{G}$ . (b) Corresponding histograms of the objective values.**

introduced in order to create a balance with the mainlobe objective. The histogram plot in Fig. 9(b) demonstrates that SA performs better on average compared to the LM method. The main reason for this is the ability of SA to leave local minima and further advance to lower minima. The convergence behavior of SA is, however, slower compared to gradient methods, such as the LM algorithm. In the above examples, including the QAOA approach, SA has been conducted with  $\mathcal{O}(10^3)$  iterations, while the LM approach required  $\mathcal{O}(10^1)$  iterations.

## VI. DISCUSSION AND CONCLUSION

Building on the above analysis of complexity and performance, it should be noted that phase-only pattern synthesis is quite demanding due to its nonlinear nature. With a circuit depth in the order of  $n_c^4 2^{4n_b}$  this means that a standard hybrid approach [2], where a classical iterative solver calls a quantum routine, would require an execution time, which is proportional to the product of the number of classical iterations times the complexity of the quantum circuit times the number of shots to determine the expectation of the problem Hamiltonian. Comparing classical optimization approaches, such as SA or gradient-based methods, to the QAOA, the execution time for phase-only pattern synthesis problems with quantum approximate optimization is longer for these demonstration examples. The analysis of an antenna example with four channels and two bit phase quantization

showed that the QAOA-approach requires a circuit with ten layers to surpass the probability of finding the global optimum with SA. Although the LM method was even better for this particular example, the analysis of a real-world example indicates that it will likely perform worse than SA for larger problem instances. However, there is a further aspect, which is related to the layer-number in quantum approximate optimization. Classically, one deals with a number of continuous optimization variables, which is the number of antenna channels  $n_c$ . The QAOA-approach optimizes over a set of continuous variables  $(\alpha_t, \beta_t)$ , which is twice the number of layers  $n_l$ . For the above example with four antenna elements this means that already with two layers the solution space of the QAOA-approach equals the size of the classical problem space.

We used higher order polynomials in the quantum approximate optimization of the phase-only pattern synthesis problem. In principle, the order of these polynomials could be reduced by introducing slack variables allowing for a reformulation of the original problem in a quadratic form. However, the reduction in the polynomial order is achieved at the cost of an increased number of variables, i.e., more qubits are needed, as well as additional constraints. The latter is a challenge, as the weights of the corresponding penalty terms need to be chosen appropriately. Poorly chosen weights can affect the problem topology in a hardly predictable manner. When it comes to the execution on real quantum annealers, another difficulty is finding a good annealing schedule, which requires a priori information on the energy gap between the ground and first excited states. Insofar quantum annealing remains a heuristic with no guarantee of finding better solutions.

Quantum approximate optimization might still be a viable option in phase-only pattern synthesis problems, specifically, if the probability to find better solutions can be increased. The analysis above showed that using more layers does indeed improve the probability to find the global optimum. One way to improve this further could be to find a better approximation of the unitary  $\exp\{-i(\alpha_t H_0 + \beta_t H_p)\}$  in the Trotterization step. This might increase the complexity of a single QAOA-layer, but potentially reduce the total number of layers and therefore even reduce the total quantum complexity.

In conclusion, this article addresses phase-only pattern synthesis in the frame of the QAOA. The key to solve this kind of classically hard to solve problem, was to introduce a quantization of the optimization variables and to write it as a combinatorial optimization problem, which is represented by a higher order polynomial. The complexity and performance analysis confirm the principal feasibility of quantum computer-assisted phase-only pattern synthesis. Although one might dispute its usefulness under the aspect of solving speed alone, the prospect of finding better solutions than classical optimization algorithms, could still render it valuable for industrial application. This, however, could require innovative modifications of the QAOA. From a general

perspective, the mathematical approach adopted in Section III, turning a nonlinear function into a finite length series, may be adopted for similar engineering problems.

## APPENDIX A

In this appendix, we fill in the steps in the calculation of the problem unitary as a result of the exponentiation of the problem Hamiltonian. Based upon the Baker–Campbell–Hausdorff formula we have

$$U_p(\beta_t) = \exp\left(-i\beta_t \sum_{i_1, i_2, \dots, i_n} c_{i_1 i_2 \dots i_n} (\sigma_1^z)^{i_1} \otimes (\sigma_2^z)^{i_2} \otimes \dots \otimes (\sigma_n^z)^{i_n}\right) \quad (40)$$

$$= \prod_{i_1, i_2, \dots, i_n} \exp\left(-i\beta_t c_{i_1 i_2 \dots i_n} (\sigma_1^z)^{i_1} \otimes (\sigma_2^z)^{i_2} \otimes \dots \otimes (\sigma_n^z)^{i_n}\right) \quad (41)$$

where the exponential of sums has been turned into a product of exponentials. Using Euler's formula and a further series expansion of the sine and cosine functions yields

$$\begin{aligned} U_p(\beta_t) &= \prod_{i_1, i_2, \dots, i_n} \left[ \cos\left(\beta_t c_{i_1 i_2 \dots i_n} (\sigma_1^z)^{i_1} \otimes (\sigma_2^z)^{i_2} \otimes \dots \otimes (\sigma_n^z)^{i_n}\right) - i \sin\left(\beta_t c_{i_1 i_2 \dots i_n} (\sigma_1^z)^{i_1} \otimes (\sigma_2^z)^{i_2} \otimes \dots \otimes (\sigma_n^z)^{i_n}\right) \right] \\ &= \prod_{i_1, i_2, \dots, i_n} \left[ \sum_{m=0}^{\infty} \frac{1}{(2m)!} \left(\beta_t c_{i_1 i_2 \dots i_n} (\sigma_1^z)^{i_1} \otimes (\sigma_2^z)^{i_2} \otimes \dots \otimes (\sigma_n^z)^{i_n}\right)^{2m} - i \sum_{m=0}^{\infty} \frac{1}{(2m+1)!} \left(\beta_t c_{i_1 i_2 \dots i_n} (\sigma_1^z)^{i_1} \otimes (\sigma_2^z)^{i_2} \otimes \dots \otimes (\sigma_n^z)^{i_n}\right)^{2m+1} \right] \\ &= \prod_{i_1, i_2, \dots, i_n} \left[ \cos\left(\beta_t c_{i_1 i_2 \dots i_n}\right) \mathbf{I} \otimes \mathbf{I} \otimes \dots \otimes \mathbf{I} - i \sin\left(\beta_t c_{i_1 i_2 \dots i_n}\right) (\sigma_1^z)^{i_1} \otimes (\sigma_2^z)^{i_2} \otimes \dots \otimes (\sigma_n^z)^{i_n} \right]. \quad (42) \end{aligned}$$

In analogy to condition (15)

$$(\sigma^z)^j = \begin{cases} \mathbf{I} & j \in 2\mathbb{N} \\ \sigma^z & j \in 2\mathbb{N} + 1 \end{cases} \quad (43)$$

has been utilized.

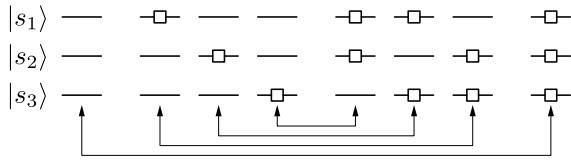


FIGURE 10. Merging concept for parallel execution of complementary subcircuits.

## APPENDIX B

The circuit depth associated with a polynomial according to (16) with all coefficients  $c_{i_1, i_2, \dots, i_n} \neq 0$  would be

$$\sum_{k=0}^n \binom{n}{k} = 2^n. \quad (44)$$

This formula suggests that all subcircuits related to terms of order  $k$  could be executed simultaneously with the subcircuits of order  $n - k$ . Note that this can be done, since all terms of the problem Hamiltonian commute. This merging concept is illustrated in Fig. 10 for  $n = 3$  qubits. The little squares indicate the qubits involved in a specific subcircuit. From this diagram it becomes clear that the reduction in circuit depth is exactly by a factor of two. In our case, when many of the coefficients  $c_{i_1, i_2, \dots, i_n}$  are zero, the additional total circuit depth reduction would be by less than a factor of two.

## REFERENCES

[1] M. Adolph et al., “High-precision temperature drift compensated T/R-module for satellite based SAR applications,” in *Proc. Eur. Microw. Conf.*, 2005, pp. 4–816, doi: [10.1109/EUMC.2005.1610050](https://doi.org/10.1109/EUMC.2005.1610050).

[2] K. Blekos et al., “A review on quantum approximate optimization algorithm and its variants,” *Phys. Rep.*, vol. 1068, pp. 1–66, 2024, doi: [10.1016/j.physrep.2024.03.002](https://doi.org/10.1016/j.physrep.2024.03.002).

[3] F. Bordoni and G. Krieger, “High-resolution wide-swath ScanSAR: Opportunities and trade-offs of a novel exploitation of radar bandwidth and PRF,” in *Proc. 13th Eur. Conf. Synthetic Aperture Radar*, 2021, pp. 1048–1051.

[4] F. G. Brandao and K. M. Svore, “Quantum speed-ups for solving semidefinite programs,” in *Proc. IEEE 58th Annu. Symp. Found. Comput. Sci.*, 2017, pp. 415–426, doi: [10.1109/FOCS.2017.45](https://doi.org/10.1109/FOCS.2017.45).

[5] G. Brown, J. Kerce, and M. Mitchell, “Extreme beam broadening using phase only pattern synthesis,” in *Proc. 4th IEEE Workshop Sensor Array Multichannel Process.*, 2006, pp. 36–39, doi: [10.1109/SAM.2006.1706079](https://doi.org/10.1109/SAM.2006.1706079).

[6] O. Bucci and G. D’Elia, “Power synthesis of reconfigurable conformal arrays with phase-only control,” *IEE Proc. - Microw. Antennas Propag.*, vol. 145, pp. 131–136, Feb. 1998, doi: [10.1049/ip-map:19981296](https://doi.org/10.1049/ip-map:19981296).

[7] O. Bucci, G. D’Elia, and G. Romito, “Synthesis technique for scanning and/or reconfigurable beam reflector antennas with phase-only control,” *IEE Proc. - Microw. Antennas Propag.*, vol. 143, pp. 402–412, Oct. 1996, doi: [10.1049/ip-map:19960262](https://doi.org/10.1049/ip-map:19960262).

[8] O. Bucci, G. D’Elia, and G. Romito, “Optimal synthesis of reconfigurable conformal arrays with phase only control,” in *Proc. IEEE Antennas Propag. Soc. Int. Symp.*, 1996, pp. 810–813, doi: [10.1109/APS.1996.549719](https://doi.org/10.1109/APS.1996.549719).

[9] A. Capozzoli, C. Curcio, G. D’Elia, and A. Liseno, “Fast phase-only synthesis of conformal reflectarrays,” *IET Microw. Antennas Propag.*, vol. 4, pp. 1989–2000, Dec. 2010, doi: [10.1049/iet-map.2009.0640](https://doi.org/10.1049/iet-map.2009.0640).

[10] A. Capozzoli, C. Curcio, G. D’Elia, A. Liseno, D. Bresciani, and H. Legay, “Fast phase-only synthesis of faceted reflectarrays,” in *Proc. 3rd Eur. Conf. Antennas Propag.*, 2009, pp. 1329–1333.

[11] F. Castella and J. Kuttler, “Optimised array antenna nulling with phase-only control,” *IEE Proc. F (Radar Signal Process.)*, vol. 138, pp. 241–246, Jun. 1991, doi: [10.1049/ip-f-2.1991.0031](https://doi.org/10.1049/ip-f-2.1991.0031).

[12] F. Castella and D. Marable, “Optimized planar array antenna nulling with phase-only control,” in *Proc. 23rd Eur. Microw. Conf.*, 1993, pp. 886–888, doi: [10.1109/EUMA.1993.336739](https://doi.org/10.1109/EUMA.1993.336739).

[13] G. Chen, H. Jiang, and X. Lei, “Reconfigurable antenna design optimization based on improved quantum genetic algorithm,” in *Proc. XXXIth URSI Gen. Assem. Sci. Symp.*, 2014, pp. 1–4, doi: [10.1109/URSIGASS.2014.6929190](https://doi.org/10.1109/URSIGASS.2014.6929190).

[14] D. Cheng, “Optimization techniques for antenna arrays,” *Proc. IEEE*, vol. 59, no. 12, pp. 1664–1674, Dec. 1971, doi: [10.1109/PROC.1971.8523](https://doi.org/10.1109/PROC.1971.8523).

[15] J. DeFord and O. Gandhi, “Phase-only synthesis of minimum peak side-lobe patterns for linear and planar arrays,” *IEEE Trans. Antennas Propag.*, vol. AP-36, no. 2, pp. 191–201, Feb. 1988, doi: [10.1109/8.1096](https://doi.org/10.1109/8.1096).

[16] E. Dufort, “Pattern synthesis based on adaptive array theory,” *IEEE Trans. Antennas Propag.*, vol. 37, no. 8, pp. 1011–1018, Aug. 1989, doi: [10.1109/8.34138](https://doi.org/10.1109/8.34138).

[17] E. Farhi, J. Goldstone, and S. Gutmann, “A quantum approximate optimization algorithm,” 2014, *arXiv:1411.4028*, doi: [10.48550/arXiv.1411.4028](https://doi.org/10.48550/arXiv.1411.4028).

[18] R. V. Gatti, L. Marcaccioli, and R. Sorrentino, “A novel phase-only method for shaped beam synthesis and adaptive nulling,” in *Proc. 33rd Eur. Microw. Conf.*, 2003, pp. 739–742, doi: [10.1109/EUMA.2003.341059](https://doi.org/10.1109/EUMA.2003.341059).

[19] N. Goto and Y. Tsunoda, “Sidelobe reduction of circular arrays with a constant excitation amplitude,” *IEEE Trans. Antennas Propag.*, vol. AP-25, no. 6, pp. 896–898, Nov. 1977, doi: [10.1109/TAP.1977.1141700](https://doi.org/10.1109/TAP.1977.1141700).

[20] L. K. Grover, “A fast quantum mechanical algorithm for database search,” in *Proc. 28th Annu. ACM Symp. Theory Comput.*, New York, NY, USA., 1996, pp. 212–219, doi: [10.1145/237814.237866](https://doi.org/10.1145/237814.237866).

[21] U. Hackenberg et al., “Polarisation agile, highly accurate T/R-module for synthetic aperture radar,” in *Proc. 33rd Eur. Microw. Conf.*, 2003, pp. 875–878, doi: [10.1109/EUMC.2003.177615](https://doi.org/10.1109/EUMC.2003.177615).

[22] S. Huber, K. Glatting, G. Krieger, and A. Moreira, “Quantum annealing for SAR system design and processing,” in *Proc. 14th Eur. Conf. Synthetic Aperture Radar*, 2022, pp. 705–710.

[23] S. Huber, Y. Wied, M. Epping, K. Glatting, and G. Krieger, “Quantum computation for SAR antenna optimization problems,” in *Proc. 15th Eur. Conf. Synthetic Aperture Radar*, 2024, pp. 1375–1380. [Online]. Available: <https://elib.dlr.de/203277/>

[24] T. Isernia, A. Massa, A. F. Morabito, and P. Rocca, “On the optimal synthesis of phase-only reconfigurable antenna arrays,” in *Proc. 5th Eur. Conf. Antennas Propag.*, 2011, pp. 2074–2077.

[25] G. Kautz, “Phase-only shaped beam synthesis via technique of approximated beam addition,” *IEEE Trans. Antennas Propag.*, vol. 47, no. 5, pp. 887–894, May 1999, doi: [10.1109/8.774152](https://doi.org/10.1109/8.774152).

[26] A. Khzmalyan and A. Kondratiev, “The phase-only shaping and adaptive nulling of an amplitude pattern,” *IEEE Trans. Antennas Propag.*, vol. 51, no. 2, pp. 264–272, Feb. 2003, doi: [10.1109/TAP.2003.809060](https://doi.org/10.1109/TAP.2003.809060).

[27] Y. Kim and R. L. Jordan, “Spaceborne SAR antennas for earth science,” 2006. [Online]. Available: [https://descanso.jpl.nasa.gov/monograph/series8/Descanso8\\_06.pdf](https://descanso.jpl.nasa.gov/monograph/series8/Descanso8_06.pdf)

[28] S. Kirkpatrick, C. D. Gelatt, and M. P. Vecchi, “Optimization by simulated annealing,” *Science*, vol. 220, no. 4598, pp. 671–680, 1983, doi: [10.1126/science.220.4598.671](https://doi.org/10.1126/science.220.4598.671).

[29] I. Krikidis, “MIMO with 1-B pre/postcoding resolution: A quantum annealing approach,” *IEEE Trans. Quantum Eng.*, vol. 5, 2024, Art. no. 2100409, doi: [10.1109/TQE.2024.3412165](https://doi.org/10.1109/TQE.2024.3412165).

[30] A. Kumar and P. Murthy, “Synthesis of equally excited linear arrays,” *IEEE Trans. Antennas Propag.*, vol. AP-25, no. 3, pp. 425–428, May 1977, doi: [10.1109/TAP.1977.1141599](https://doi.org/10.1109/TAP.1977.1141599).

[31] J. Liang, X. Fan, W. Fan, D. Zhou, and J. Li, “Phase-only pattern synthesis for linear antenna arrays,” *IEEE Antennas Wireless Propag. Lett.*, vol. 16, pp. 3232–3235, 2017, doi: [10.1109/LAWP.2017.2771380](https://doi.org/10.1109/LAWP.2017.2771380).

[32] Q. J. Lim, C. Ross, A. Ghosh, F. W. Vook, G. Gradoni, and Z. Peng, “Quantum-assisted combinatorial optimization for reconfigurable intelligent surfaces in smart electromagnetic environments,” *IEEE Trans. Antennas Propag.*, vol. 72, no. 1, pp. 147–159, Jan. 2024, doi: [10.1109/TAP.2023.3298134](https://doi.org/10.1109/TAP.2023.3298134).

- [33] S.-M. Lin, Y.-Q. Wang, and P.-L. Shen, "Phase-only synthesis of the shaped beam patterns for the satellite planar array antenna," in *Proc. IEEE Int. Conf. Phased Array Syst. Technol.*, 2000, pp. 331–334, doi: [10.1109/PAST.2000.858968](https://doi.org/10.1109/PAST.2000.858968).
- [34] M. Ma, "Linear arrays with non-uniform progressive phase shift," in *Proc. IRE Int. Conv. Rec.*, 1963, pp. 70–76, doi: [10.1109/IRECON.1963.1147178](https://doi.org/10.1109/IRECON.1963.1147178).
- [35] K. Madsen, H. B. Nielsen, and O. Tingleff, "Methods for non-linear least squares problems (2nd ed.)," *Inf. Math. Modelling*, Tech. Univ. Denmark, DTU, 2004, Art. no. 60.
- [36] N. Metropolis, A. W. Rosenbluth, M. N. Rosenbluth, A. H. Teller, and E. Teller, "Equation of state calculations by fast computing machines," Los Alamos Scientific Lab., Los Alamos, NM, USA, Tech. Rep. LA-UR-53-231, Mar. 1953, doi: [10.1063/1.1699114](https://doi.org/10.1063/1.1699114).
- [37] S. Mikki and A. Kishk, "Quantum particle swarm optimization for electromagnetics," *IEEE Trans. Antennas Propag.*, vol. 54, no. 10, pp. 2764–2775, Oct. 2006, doi: [10.1109/TAP.2006.882165](https://doi.org/10.1109/TAP.2006.882165).
- [38] J. J. Moré, "The Levenberg-Marquardt algorithm: Implementation and theory," in *Proc. Numer. Anal.*, 1978, pp. 105–116, doi: [10.1007/BFb0067700](https://doi.org/10.1007/BFb0067700).
- [39] V.-V. Nguyen, H. Nam, Y. J. Choe, B.-H. Lee, and J.-D. Park, "An X-band bi-directional transmit/receive module for a phased array system in 65-nm CMOS," *Sensors*, vol. 18, no. 8, 2018, Art. no. 2569, doi: [10.3390/s18082569](https://doi.org/10.3390/s18082569).
- [40] M. A. Nielsen and I. L. Chuang, *Quantum Computation and Quantum Information: 10th Anniversary Edition*. Cambridge, U.K.: Cambridge Univ. Press, 2010, doi: [10.1017/CBO9780511976667](https://doi.org/10.1017/CBO9780511976667).
- [41] E. Pelofske, A. B4rtschi, and S. Eidenbenz, "Short-depth QAOA circuits and quantum annealing on higher-order ising models," *npj Quantum Inf.*, vol. 10, Mar. 2024, Art. no. 30, doi: [10.1038/s41534-024-00825-w](https://doi.org/10.1038/s41534-024-00825-w).
- [42] B. Pompeo, L. Pralon, M. Pralon, and R. Mendes, "Phase-only pattern synthesis using a modified least squares method for phased arrays," in *Proc. Eur. Microw. Conf.*, 2013, pp. 1755–1758, doi: [10.23919/EuMC.2013.6687017](https://doi.org/10.23919/EuMC.2013.6687017).
- [43] R. J. Reinke, D. Schwartzman, F. Nai, T.-Y. Yu, J. Salazar-Cerreno, and R. D. Palmer, "Evaluation of a spline-based parameterization scheme for phase-only antenna pattern synthesis," in *Proc. IEEE Int. Symp. Phased Array Syst. Technol.*, 2022, pp. 1–8, doi: [10.1109/PAST49659.2022.9975004](https://doi.org/10.1109/PAST49659.2022.9975004).
- [44] P. Rocca, N. Anselmi, G. Oliveri, A. Polo, and A. Massa, "Antenna array thinning through quantum Fourier transform," *IEEE Access*, vol. 9, pp. 124313–124323, 2021, doi: [10.1109/ACCESS.2021.3109938](https://doi.org/10.1109/ACCESS.2021.3109938).
- [45] C. Ross, G. Gradoni, Q. J. Lim, and Z. Peng, "Engineering reflective metasurfaces with ising Hamiltonian and quantum annealing," *IEEE Trans. Antennas Propag.*, vol. 70, no. 4, pp. 2841–2854, Apr. 2022, doi: [10.1109/TAP.2021.3137424](https://doi.org/10.1109/TAP.2021.3137424).
- [46] F. Rostan et al., "ROSE-L SAR instrument design overview and performance," in *Proc. 15th Eur. Conf. Synthetic Aperture Radar*, 2024, pp. 209–214.
- [47] S. Smith, "Optimum phase-only adaptive nulling," *IEEE Trans. Signal Process.*, vol. 47, no. 7, pp. 1835–1843, Jul. 1999, doi: [10.1109/78.771033](https://doi.org/10.1109/78.771033).
- [48] M. Stangl, R. Werninghaus, and R. Zahn, "The TerraSAR-X active phased array antenna," in *Proc. IEEE Int. Symp. Phased Array Syst. Technol.*, 2003, pp. 70–75, doi: [10.1109/PAST.2003.1256959](https://doi.org/10.1109/PAST.2003.1256959).
- [49] A. Stockley and K. Briggs, "Optimizing antenna beamforming with quantum computing," in *Proc. 17th Eur. Conf. Antennas Propag.*, 2023, pp. 1–5, doi: [10.23919/EuCAP57121.2023.10133700](https://doi.org/10.23919/EuCAP57121.2023.10133700).
- [50] L. Tosi and P. Rocca, "A quantum optimization method for antenna array thinning," in *Proc. 18th Eur. Conf. Antennas Propag.*, 2024, pp. 1–4, doi: [10.23919/EuCAP60739.2024.10501035](https://doi.org/10.23919/EuCAP60739.2024.10501035).
- [51] L. Tosi, P. Rocca, N. Anselmi, and A. Massa, "Array-antenna power-pattern analysis through quantum computing," *IEEE Trans. Antennas Propag.*, vol. 71, no. 4, pp. 3251–3259, Apr. 2023, doi: [10.1109/TAP.2023.3242128](https://doi.org/10.1109/TAP.2023.3242128).
- [52] A. Trastoy and F. Ares, "Phase-only synthesis of continuous linear aperture distribution patterns with asymmetric side lobes," *Electron. Lett.*, vol. 34, no. 20, pp. 1916–1917, Oct. 1998, doi: [10.1049/el:19981340](https://doi.org/10.1049/el:19981340).
- [53] M. Younis, F. Q. D. Almeida, M. Villano, S. Huber, G. Krieger, and A. Moreira, "Digital beamforming for spaceborne reflector-based synthetic aperture radar, part 2: Ultrawide-swath imaging mode," *IEEE Geosci. Remote Sens. Mag.*, vol. 10, no. 4, pp. 10–31, Dec. 2022, doi: [10.1109/MGRS.2022.3200871](https://doi.org/10.1109/MGRS.2022.3200871).
- [54] S. S. A. Yuan et al., "Quantum annealing-inspired optimization for space-time coding metasurface," *IEEE Trans. Antennas Propag.*, vol. 73, no. 9, pp. 6512–6524, Sep. 2025, doi: [10.1109/TAP.2025.3573526](https://doi.org/10.1109/TAP.2025.3573526).



**Sigurd Huber** received the M.S. degree in electrical and communication engineering from the Technical University of Munich (TUM), Munich, Germany, in 2005, and the Ph.D. (Hons.) degree in electrical and communication engineering from the Karlsruhe Institute of Technology, Karlsruhe, Germany, in 2014.

Since 2005, he has been with the Microwaves and Radar Institute of the German Aerospace Center, Oberpfaffenhofen, Germany, where he is engaged in the conception of future synthetic aperture radar systems utilizing advanced multichannel antenna architectures. He is involved in national and international projects in the field of Earth observation, encompassing collaborations with industry partners (Airbus, OHB, and Hensoldt), as well as research organizations (ESA, NASA/JPL, and JAXA). For the German Earth observation mission proposal Tandem-L, he was responsible for synthetic aperture radar system and performance engineering. In 2018 to 2019, he was a Project Manager for the Phase A and Phase B1 studies of the mission proposal ROSE-L within the framework of ESA's Copernicus programme. Since 2021, he has been heading a team of quantum researchers with a focus on applications of quantum computing in the field of radar remote sensing. He has authored or coauthored more than 100 publications in international conferences and journals and is the holder of patents on array-fed reflector antennas for synthetic aperture radar applications, as well as on a Grover search-based approach to phase-only pattern synthesis. His research interests include classical and quantum field theory and, more specifically, digital signal processing, inverse problems, array processing, antenna theory, quantum optics, and quantum computing.



**Michael Epping** was born in Arnsberg, Germany, in 1987. He received the B.Sc. degree in physics from the University of Siegen, Siegen, Germany, in 2010, the M.Sc. degree in theoretical and mathematical physics from the University of Vienna, Vienna, Austria, in 2012, and the Ph.D. degree in theoretical and mathematical physics from the Heinrich-Heine-University Düsseldorf, Düsseldorf, Germany, in 2015.

He worked with the Heinrich-Heine-University of Düsseldorf, the Institute for Quantum Computing, Waterloo, ON, Canada, and at dSPACE GmbH, Paderborn, Germany. Since 2021, he has been with the Institute of Software Technology, German Aerospace Center, Cologne, Germany where he leads a research group on quantum computing. His research interests include quantum computing, quantum error correction, compilation of quantum algorithms, and quantum communication.